U.S. Department of Energy
Office of River Protection
P.O. Box 450, MSIN H6-60
Richland, Washington 99352

12-WTP-0216

JUL 17 2012

The Honorable Peter S. Winokur
Chairman
Defense Nuclear Facilities Safety Board
625 Indiana Avenue, NW, Suite 700
Washington. DC 20004-2901

Dear Mr. Chairman:

TRANSMITTAL OF DEFENSE NUCLEAR FACILITIES SAFETY BOARD (DNFSB) RECOMMENDATION 2010-2 IMPLEMENTATION PLAN (IP) DELIVERABLES 5.3.3.1 AND CANCELLATION OF 5.3.3.2 AND 5.3.3.3

This letter provides the deliverable responsive to Commitment 5.3.3.1 of the U.S. Department of Energy plan to address Waste Treatment and Immobilization Plant (WTP) Vessels Mixing Issues; IP for DNFSB 2010-2. Follow-on Commitments 5.3.3.2 and 5.3.3.3 will be cancelled based on conclusions reached in 5.3.3.1.

The attached report provides experimental results of a non-Newtonian proof of concept scoping test. The report assessed the use of Newtonian analytical techniques to assess mixing in non-Newtonian vessels. Results of the test suggest that the premise that non-Newtonian fluids perform the same as matched Newtonian fluids under appropriately similar conditions is not supported. Report conclusions indicate that extensive additional testing might be required, with no clear route to success. Based on these conclusions, it has been determined that Newtonian techniques will not be utilized for analysis of non-Newtonian vessel performance.

Determination that Newtonian techniques will not be utilized has resulted in the cancellation of 24590-WTP-RPT-ENG-11-001, Rev 0, "Determination that Non-Newtonian Vessels Can Be Evaluated Using Newtonian Techniques." Report cancellation and determination from the proof of concept scoping test report are intended to fulfill the requirements of IP Commitment 5.3.3.1, update assessment of use of Newtonian analysis techniques to assess non-Newtonian vessel performance.

Subsequent efforts in support of IP Commitment 5.3.3.2, independent review of paper concluding non-Newtonian conditions can be assessed using Newtonian techniques and 5.3.3.3, conclusion regarding use of Newtonian techniques to assess non-Newtonian conditions are being cancelled. Alternative approaches will be used to complete analysis for non-Newtonian vessel performance. These approaches will be considered in preparing the revised IP due to be completed by the end of this calendar year.

If you have any questions, please contact me at (509) 372-2315, or your staff may contact Ben Harp, WTP Start-up and Commissioning Integration Manager at (509) 376-1462.

Sincerely,

Scott L. Samuelson, Manager
Office of River Protection

WTP:WRW

Attachments

cc w/attachs:
D. M. Busche, BNI
W. W. Gay, BNI
F. M. Russo, BNI
D. McDonald, Ecology
D. G. Huizenga, EM-1
M. B. Moury, EM-1
T. P. Mustin, EM-1
K. G. Picha, EM-1
C. S. Trummell, EM-1
A. C. Williams, EM-2.1
J. D. Lorence, EM-41
D. Chung, HS-1
M. N. Campagnone, HS-1.1
R. H. Lagdon, Jr., US
M. D. Johnson, WRPS
S. A. Saunders, WRPS
R. G. Skwarek, WRPS
M. G. Thien, WRPS
BNI Correspondence
WRPS Correspondence

Attachment 1
To
12-WTP-0216

TRANSMITTAL OF DEFENSE NUCLEAR FACILITIES SAFETY BOARD (DNFSB) RECOMMENDATION 2010-2 IMPLEMENTATION PLAN (IP) DELIVERABLES 5.3.3.1 AND CANCELLATION OF 5.3.3.2 AND 5.3.3.3

Non-Newtonian Proof of concept Scoping Test Report

Pages: 37 (including Coversheet)

Non-Newtonian Proof of Concept Scoping Test Report

Document title:

Document number: 24590-WTP-RPT-ENG-11-164, Rev 0

Contract number: DE-AC27-01RV14136

Department: Vessel Completion Team Engineering

Author(s): Joel Peltier
Beric Wells - PNNL
Dave Rector - PNNL

Checked by: Robert Hanson

Issue status: Approved

Approved by: Russell Daniel

Approver's position: VCT Technical Manager

Approver's signature: Russell D Daniel (Signature) 5/24/12 (Date)

River Protection Project
Waste Treatment Plant
2435 Stevens Center Place
Richland, WA 99354
United States of America
Tel: 509 371 2000

History Sheet

Rev	Reason for revision	Revised by
0	Approved	J Peltier

Contents

Appendices

Tables

Figures

Acronyms

ECR	Effective Clearing Radius
NB	Newtonian Bed
NNB	non-Newtonian Bed
NJ	Newtonian Jet
NNJ	non-Newtonian Jet
NQA	Nuclear Quality Assurance
PJM	pulse jet mixer
WTP	Hanford Tank Waste Treatment and Immobilization Plant
ZOI	zone of influence

Symbols

Cs	Volume fraction of the solids
D	nozzle diameter
ECR	effective clearing radius
d_a	arithmetic mean diameter of the particles in the mixture bed
g	acceleration of gravity
H	nozzle offset height
K	kinematic momentum flux
r	radial distance from jet
s_a	submerged specific weight based on the arithmetic-average density)
UCS	unconfined compressive strength of the cohesive mixture
e	void ratio of the mixture bed (volume of liquid/volume of solids)
Pc	weight fraction of clay (fines) in the mixture bed
Re_p	particle Reynolds number based upon U_g
U	nozzle (jet) velocity
U_g	characteristic velocity for particle settling ($U_g=s_a\ g\ d_a$)

Greek Symbols

γ	shear rate
ρ	density of the jet fluid
ρ_l	density of the liquid
ρ_s	density of the slurry
θ_c	critical Shields parameter for mobilization of a non-cohesive particle bed
τ	shear stress
τ_0	initial shear stress/ Bingham fluid yield stress

τ_c	critical shear stress to mobilize a non-cohesive particle of diameter d_a
τ_{cc}	critical shear stress to mobilize the cohesive mixture bed
$\tau_{S,N}$	shear strengths of the Newtonian bed
$\tau_{S,NN}$	ₛhear strengths of the non-Newtonian bed
τ_w	wall shear stress
μ_l	dynamic liquid viscosity
ν_l	kinematic liquid viscosity
ν	kinematic viscosity of jet fluid

Executive Summary

The Test 5 scoping study was authorized to allow a rapid evaluation of the experimental design before NQA-1 data were collected. Phase 1 of the scoping tests collected data for a single pulse tube configuration, as they would be collected in actual Test 5 Phase 1 runs. These data clearly indicated an endemic problem with the Test 5 design of experiment and the pass/fail criteria for the experiment with respect to answering the question as to whether a sufficiently sheared Bingham fluid may be analyzed using Newtonian flow assumptions. A decision was made not to continue to Test 5 Phase 2 scoping runs and to not proceed with Test 5 NQA-1 data collection.

Analyses are documented in this report which show that the Test 5 scoping run data 1) may be consistent with the concept that "a sufficiently sheared Bingham fluid may be analyzed using Newtonian flow assumptions" but that 2) the pretest assumed relationship between the unconfined compressive strength of the Test 5 bed modeled as a factor of 2 to 2.3 times that Bingham fluid yield stress was not valid. Evidence is presented that suggests the unconfined compressive strength of the Test 5 bed may be many orders of magnitude larger than the pretest estimate. The Test 5 scoping run data are inconclusive in establishing whether the Test 5 experiment could show whether a sufficiently sheared Bingham fluid may be analyzed using Newtonian flow assumptions if Test 5 bed properties were suitably characterized. Because it was determined that extensive additional testing and development of new measurement and analysis techniques might be required to yield a successful Test 5 experiment, with no clear route to success, it was decided that Newtonian techniques will not be used to assess non-Newtonian vessel performance and that 24590-WTP-RPT-ENG-11-001, Rev 0. 2011, *Determination that Non-Newtonian Vessels Can Be Evaluated Using Newtonian Techniques*, which provided the basis for the assumption, will be cancelled.

1 Background

Data comparisons of jet-mixing performance for Non-Newtonian Hanford fluids versus Newtonian Hanford fluids are limited. While jet-mixing performance data have been reported (24590-WTP-RPT-ENG-11-001, Rev 0, *Determination That Non-Newtonian Vessels Can Be Evaluated Using Newtonian Techniques*) covering ranges of fluid properties and various suspended or settling solids, a direct one-for-one comparison of properties of concern to Pulse Jet Mixing using Newtonian fluid and a Non-Newtonian fluid has not been conducted for Hanford Tank Wastes. Specifically, comparison of yield stress fluids with infinite strain-rate viscosities in terms of radial wall jet clearing of a bed of solids to Newtonian fluids with similar viscosity was needed.

A test plan was formed (CCN 238153, *Testing Associated With The Determination That Non-Newtonian Vessels Can Be Evaluated Using Newtonian Techniques*) with the objective to use measurement of clearing radius of a bed of solids to demonstrate whether a Non-Newtonian yield stress fluid performs the same as a Newtonian fluid surrogate under appropriately similar conditions. These tests were called Test 5. Test 5 was to be conducted in two phases. Phase 1 considers a single jet impinging on a bed of solids with the intent to show that the non-Newtonian fluid acts as a Newtonian fluid in its interaction with the solids bed. Phase 2 considers multiple jets with the intent to show that the non-Newtonian fluid acts as a Newtonian fluid at mean velocity stagnation points. Phase 2 would be conducted only upon successful completion of Phase 1.

Scoping tests for Test 5 were authorized to allow a rapid evaluation of the experimental design before NQA-1 data were collected in Phase 1. Details of the scoping apparatus and test results are reported in project document 24590-RMCD-03354, *Summary of LSIT-Info-N-NN-ECR-005 & 5a, Phase I: Single PJM, Determination If Non-Newtonian Vessels Can Be Evaluated Using Newtonian Techniques Using 0.25-In. Bed Depth.* This report is an analysis of scoping test data.

2 Purpose

The purpose of Test 5 is to supplement the findings of project report 24590-WTP-RPT-ENG-11-001, Rev 0, *Determination That Non-Newtonian Vessels Can Be Evaluated Using Newtonian Techniques*, specifically to assess whether the premise that non-Newtonian fluids perform the same as matched Newtonian fluids under appropriately similar conditions may be supported.

The purpose of the Test 5 Scoping Study was to allow a rapid evaluation of the experimental design of Test 5, before NQA-1 data were collected, in order to learn whether the objective to use measurement of clearing radius of a bed of solids to demonstrate whether a Non-Newtonian yield stress fluid performs the same as a Newtonian fluid surrogate under appropriately similar conditions could be successful. Successful scoping test runs would allow the Test 5 experiment to proceed. Unsuccessful scoping test runs could be used to identify issues with the Test 5 experiment design that need to be addressed in order to enable Test 5 to evaluate that premise.

3 Results

A complete summary of the Test 5 Scoping Study data is provided in project document 24590-RMCD-03354, *Summary of LSIT-Info-N-NN-ECR-005 & 5a, Phase I: Single PJM, Determination If Non-*

Newtonian Vessels Can Be Evaluated Using Newtonian Techniques Using 0.25-In. Bed Depth. The Zone of Influence (ZOI) data from Newtonian Jets (NJ) impinging on Newtonian settled solids beds (NB) (Figure 1), non-Newtonian Jets (NNJ) impinging on non-Newtonian settled solids beds (NNB) (Figure 2), Newtonian Jets impinging on non-Newtonian settled solids beds (Figure 3), and non-Newtonian Jets impinging on Newtonian settled solids beds (Figure 4) are extracted from that report.

Bed and Jet Type	Pulse	Ave. Vel, m/s	Vel Last 3, s m/s	Dia, cm
NB-NJ	1	6.16	6.06	46.17
NB-NJ	2	6.11	6.00	51.07
NB-NJ	3	5.96	5.81	46.87
NB-NJ	4	6.23	6.09	48.18
NB-NJ	5	6.01	5.87	46.73
NB-NJ	6	5.98	5.86	46.83
NB-NJ	7	6.04	5.92	46.60
NB-NJ	8	6.09	5.93	48.08
NB-NJ	9	6.15	6.01	51.73
NB-NJ	10	6.20	6.07	51.79
Ave			5.96	48.40
Stddev			0.1	2.25
% Rel Stddev			1.7	4.65

Figure 1 **Clearing diameters (ZOI) from the Test 5 Scoping Study for Newtonian Jets impinging on Newtonian settled solids beds for pulses within 0.2m/s of 6m/s during the last three seconds of the pulse.**

Bed and Jet Type	Pulse	Ave. Vel, m/s	Vel Last 3, s m/s	Dia, cm
NNB-NNJ	2E	6.13	6.03	24.31
NNB-NNJ	3	6.26	6.13	26.25
NNB-NNJ	4	6.11	5.95	28.22
NNB-NNJ	5	6.01	5.87	26.52
NNB-NNJ	6	6.06	5.90	24.20
NNB-NNJ	7	6.19	6.04	27.19
NNB-NNJ	8	6.22	6.04	25.58
NNB-NNJ	12	6.18	6.05	24.84
NNB-NNJ	15	6.11	5.94	24.56
Ave			5.99	25.74
Stddev			0.08	1.40
% Rel Stddev			1.39	5.46

Figure 2 **Clearing diameters (ZOI) from the Test 5 Scoping Study for non-Newtonian Jets impinging on non-Newtonian settled solids beds for pulses within 0.2m/s of 6m/s during the last three seconds of the pulse.**

Bed and Jet Type	Pulse	Ave. Vel m/s	Vel Last 3 s m/s	Dia, cm
NNB-NJ	1	6.1	5.95	28.96
NNB-NJ	2B	6.18	6.09	29.13
NNB-NJ	3	6.09	5.97	30.44
NNB-NJ	4	5.88	5.77	30.28
NNB-NJ	4A	6.22	6.1	32.60
NNB-NJ	5	6.66	6.58	34.57
NNB-NJ	6	6.33	6.23	32.39
NNB-NJ	7	5.81	5.65	29.99
NNB-NJ	7A	5.79	5.63	31.33
NNB-NJ	7B	6.22	6.09	31.32
NNB-NJ	9	6.13	6.12	29.91
NNB-NJ	10	6.11	5.96	29.17
NNB-NJ	12	5.91	5.78	29.39
NNB-NJ	13	6.1	5.97	29.60
NNB-NJ	14	6.06	5.91	30.38
Ave			5.99	30.63
Stddev			0.24	1.57
% Rel Stddev			4.00	5.12

Figure 3 **Clearing diameters (ZOI) from the Test 5 Scoping Study for Newtonian Jets impinging on non-Newtonian settled solids beds for pulses within 0.2m/s of 6m/s during the last three seconds of the pulse.**

Bed and Jet Type	Pulse	Ave. Vel, m/s	Dia, cm
NB-NNJ	1	5.96	30.8
NB-NNJ	1	5.98	29.8
Ave		5.97	30.3

Figure 4 **Clearing diameters (ZOI) from the Test 5 Scoping Study for non-Newtonian Jets impinging on Newtonian settled solids beds.**

Average values for the cleared zone diameters are

- 48.40 cm ± 2.25 cm, for Newtonian jet clearing of a Newtonian settled solids bed
- 25.74 cm ± 1.40 cm, for non-Newtonian jet clearing of a non-Newtonian settled solids bed
- 30.63 cm ± 1.57 cm, for Newtonian jet clearing of a non-Newtonian settled solids bed
- 30.30 cm ± unknown, for non-Newtonian jet clearing of a Newtonian settled solids bed

A summary of clearing zone diameters for all Test 5 Scoping Study runs is presented in Figure 5, expressed in terms of the effective clearing (or cleaning) radius (ECR) defined as one-half of the cleared zone diameter. The data were extracted from project document project document 24590-RMCD-03354, *Summary of LSIT-Info-N-NN-ECR-005 & 5a, Phase I: Single PJM, Determination If Non-Newtonian Vessels Can Be Evaluated Using Newtonian Techniques Using 0.25-In. Bed Depth.*

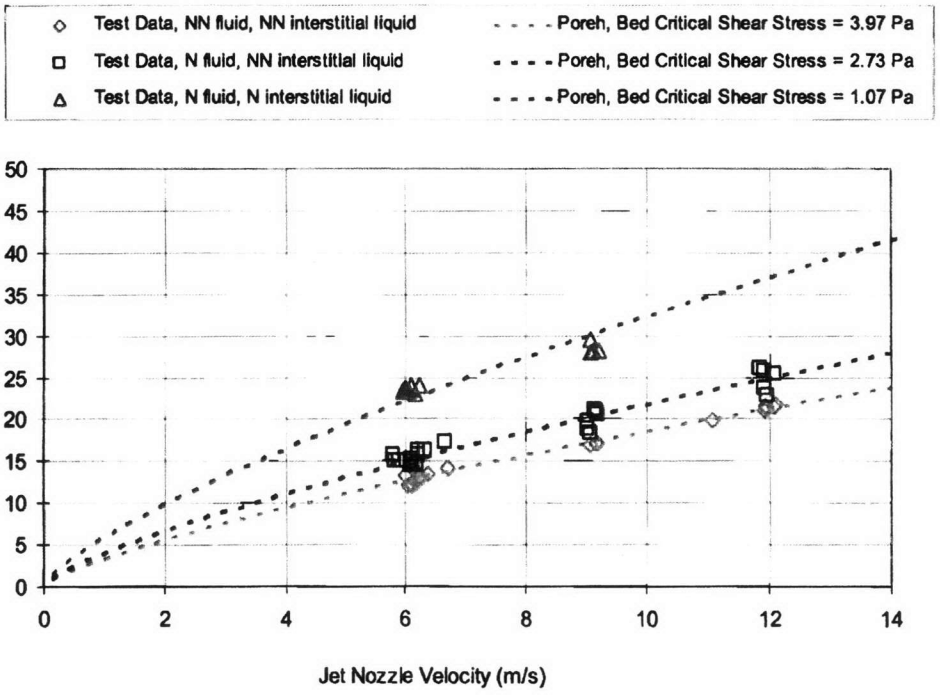

Figure 5 **Summary of ECR (1/2 of the Clearing Diameter) data for all Test 5 Scoping Study Runs.**

4 Analysis

4.1 Test 5 Analysis Approach

The analysis approach advocated in the Test 5 plan (CCN 238153, *Testing Associated With The Determination That Non-Newtonian Vessels Can Be Evaluated Using Newtonian Techniques*) is to compare the experimentally observed clearing diameters for the NB-NJ and NNB-NNJ runs.

- Success: If the observed average clearing diameter from the NNB-NNJ runs was the same as or exceeded the observed average clearing diameter from the NB-NJ runs under appropriately matched conditions, then the experiment would be successful in supporting the premise that non-

Newtonian fluids perform the same as matched Newtonian fluids under appropriately similar conditions. The experiments would proceed to Phase 2.

- If the observed average clearing diameter from the NNB-NNJ runs was less than the observed average clearing diameter from the NB-NJ runs under appropriately matched conditions, then the experimentally observed average clearing diameter for the NNB-NNJ runs would be modified by the ratio of the predicted NB-NJ clearing diameter to the predicted NNB-NNJ clearing diameter to adjust for fluid and bed differences and the comparison would be repeated.
  - Success: If the adjusted average clearing diameter from the NNB-NNJ runs was the same as or exceeded the observed average clearing diameter from the NB-NJ runs under appropriately matched conditions, then the experiment would be successful in supporting the premise that non-Newtonian fluids perform the same as matched Newtonian fluids under appropriately similar conditions. The experiments would proceed to Phase 2.
  - Failure: If the adjusted average clearing diameter from the NNB-NNJ runs was less than the observed average clearing diameter from the NB-NJ runs under appropriately matched conditions, then the experiment would be interpreted to not support the premise that non-Newtonian fluids perform the same as matched Newtonian fluids under appropriately similar conditions.

The observed value for the average clearing diameter from the nominally 6 m/s NNB-NNJ runs, 25.74 cm ± 1.40 cm, is substantially less than the observed value for the average clearing diameter from the nominally 6 m/s NB-NJ runs, 48.40 cm ± 2.25 cm, thereby requiring a comparison to the adjusted NNB-NNJ value.

4.2 NNB-NNJ Adjustment

The Test 5 analysis plan recommends use of the ECR model

$$ECR = \left[0.244 \rho_l U^{1.7} \tau_c^{-1} \left(\frac{D}{H} \right)^2 \left(\frac{\nu_l}{D} \right)^{0.3} \right]^{0.435} H \qquad \text{Equation 1}$$

where
- ECR = radial distance from the jet (m)
- U = impinging jet nozzle velocity (m/s)
- τ_c = critical shear stress to mobilize the settled solids bed (Pa)
- ρ_l = density of jet fluid (kg/m^3)
- H = jet nozzle offset from the floor (m)
- D = jet nozzle diameter (m)
- ν = kinematic viscosity of jet fluid (m^2/s)

For the Test 5 Scoping Study experiments, D = 1/2 inch = 0.0127 m and H/D = 1.5.

4.2.1 NB-NJ Tests

The measured carrier fluid density and viscosity for the Newtonian fluid tests are $\rho_l = \rho_{glycerol} = 1158$ kg/m^3 and $\mu_{glycerol} = 10.88$ cP = 0.01088 kg /(m s) (see appendix A.1). The kinematic viscosity of the carrier fluid is $\mu_l/\rho_l = 9.396 \times 10^{-6}$ m^2/s. The average nozzle velocity for the NB-NJ tests is U = 5.96 m/s (Figure 1). The critical shear stress for mobilization is predicted to be $\tau_c = 0.7956$ Pa using the Brownlie (1981) model for the Shields relations (see appendix A.4 for calculation) and $\tau_c = 0.9838$ Pa using the

Cao et al. (2006) model for the Shields relations (see appendix A.5). Using these data, the predicted value for ECR based on Brownlie (1981) is

$$ECR = \left[0.244\rho_l U^{1.7}\tau_c^{-1}\left(\frac{D}{H}\right)^2\left(\frac{\nu_l}{D}\right)^{0.3}\right]^{0.435} H$$

$$= \left[0.244 \cdot 1158 \cdot 5.96^{1.7} \cdot 0.7956^{-1} \cdot \left(\frac{0.0127}{0.01905}\right)^2 \cdot \left(\frac{9.936\times10^{-6}}{0.0127}\right)^{0.3}\right]^{0.435} 0.01905m$$

$$= 0.2517m$$

and based on the Cao et al. (2006) is

$$ECR = \left[0.244\rho_l U^{1.7}\tau_c^{-1}\left(\frac{D}{H}\right)^2\left(\frac{\nu_l}{D}\right)^{0.3}\right]^{0.435} H$$

$$= \left[0.244 \cdot 1158 \cdot 5.96^{1.7} \cdot 0.9838^{-1} \cdot \left(\frac{0.0127}{0.01905}\right)^2 \cdot \left(\frac{9.936\times10^{-6}}{0.0127}\right)^{0.3}\right]^{0.435} 0.01905m$$

$$= 0.2295m$$

The predicted diameter of the cleared zone is 2xECR which is 50.33 cm for the Brownlie (1981) model and 45.89 cm for the Cao et al. (2006). The average of the measured values is 48.40 cm ± 2.25 cm (Figure 1). The Brownlie (1981) prediction lies at the upper end of this range. The Cao et al. (2006) prediction lies at the lower end of this range.

4.2.2 NNB-NNJ Tests

The measured carrier fluid density and viscosity for the Newtonian fluid tests are $\rho_l = \rho_{slurry} = 1200$ kg/m^3 and $\mu_l = \mu_{\infty,Slurry} = 11.3$ cP = 0.0113 kg/ms (see appendix A.2). The kinematic viscosity of the carrier fluid is $\mu_l/\rho_l = 9.417\text{x}10^{-6}$ m^2/s. The average nozzle velocity for the NNB-NNJ tests is U = 5.99 m/s (Figure 2). The critical shear stress for mobilization of the cohesive bed is predicted to be $\tau_{cc} = 0.995$ Pa using the Brownlie (1981) model for the Shields relations augmented by the Kothyari and Jain (2008) model for bed cohesion (see appendix A.7 for calculation) and $\tau_{cc} = 1.246$ Pa using the Cao et al. (2006) model for the Shields relations similarly augmented by the Kothyari and Jain (2008) model for bed cohesion (see appendix A.8). Using these data, the predicted value for ECR based on Brownlie (1981) is

$$ECR = \left[0.244\rho_l U^{1.7}\tau_{cc}^{-1}\left(\frac{D}{H}\right)^2\left(\frac{\nu_l}{D}\right)^{0.3}\right]^{0.435} H$$

$$= \left[0.244 \cdot 1200 \cdot 5.99^{1.7} \cdot 0.995^{-1} \cdot \left(\frac{0.0127}{0.01905}\right)^2 \cdot \left(\frac{9.417\times10^{-6}}{0.0127}\right)^{0.3}\right]^{0.435} 0.01905m$$

$$= 0.2328m$$

and based on the Cao et al. (2006) is

$$ECR = \left[0.244\rho_l U^{1.7}\tau_{cc}^{-1}\left(\frac{D}{H}\right)^2\left(\frac{\nu_l}{D}\right)^{0.3}\right]^{0.435} H$$

$$= \left[0.244 \cdot 1200 \cdot 5.99^{1.7} \cdot 1.246^{-1} \cdot \left(\frac{0.0127}{0.01905}\right)^2 \cdot \left(\frac{9.417\times10^{-6}}{0.0127}\right)^{0.3}\right]^{0.435} 0.01905m$$

$$= 0.2111m$$

The predicted diameter of the cleared zone is 2xECR which is 46.57 cm for the Brownlie (1981) model and 42.23 cm for the Cao et al. (2006). The average of the measured values is 25.74 cm ± 1.40 cm (Figure 1). Both the Brownlie (1981) and Cao et al. (2006) predictions lie significantly outside of this range.

4.2.3 Adjustment

Following the analysis strategy proposed in the Test 5 plan, the observed value for clearing diameter from the NNB-NNJ tests, 25.74 cm, is adjusted by the ratio of the predicted clearing diameter for the NB-NJ test, 50.33 cm for the Brownlie (1981) model and 45.89 cm for the Cao et al. (2006), to the predicted clearing diameter for the NNB-NNJ test, 46.57 cm for the Brownlie (1981) model and 42.23 cm for the Cao et al. (2006). The adjustment ratios are 50.3/46.57 = 1.08 based on the Brownlie (1981) model and 1.09 based on the Cao et al. (2006) model. The adjusted values for the average clearing diameter for the NNB-NNJ tests are 1.08 x 25.74 cm = 27.8 cm based on the Brownlie (1981) model and 28.1 cm based on the Cao et al. (2006) model.

Both of these adjusted values, 27.8 cm and 28.1 cm, remain considerably below the observed value of 48.4 cm for the NB-NJ runs.

4.3 Summary

The results of the Test 5 Scoping Study following the analysis strategy proposed in the Test 5 plan would suggest that the premise that non-Newtonian fluids perform the same as matched Newtonian fluids under appropriately similar conditions is not supported. The other possibility is that the Test 5 Scoping Study has uncovered a flaw in the Test 5 experimental design that would preclude the ability of the Test 5 experiment to assess whether non-Newtonian fluids perform the same as matched Newtonian fluids under appropriately similar conditions.

4.4 Estimating the Critical Stress for Erosion

Estimates of the critical stress to erode the Newtonian and non-Newtonian interstitial fluid beds with the different fluid jets are made and the results for the different fluid and bed interactions are compared. Estimates for the critical stress based on empirical models from the literature (e.g. Kothyari and Jain 2008) for the non-Newtonian bed, see Section 3) are also provided and compared.

The critical stress to erode the beds is estimated from the measured ECR as a function of jet nozzle velocity using the Poreh et al. (1967) expression for the wall shear stress acting on the floor from an impinging radial jet, τ_w, as

$$\tau_w = \frac{0.3\rho K}{H^2}\left(\frac{\sqrt{K}}{\nu}\right)^{-0.3}\left(\frac{r}{H}\right)^{-2.3} \qquad \text{Equation 2}$$

where
- r = radial distance from the jet
- τ_w = wall shear stress
- ρ = density of jet fluid (kg/m^3)
- K = kinematic momentum flux from the jet nozzle (m^4/s^2), $K = \frac{\pi}{4}(U_0 D_0)^2$ where U_0 and D_0 are the jet nozzle velocity and diameter respectively
- H = nozzle stand-off distance for vessel bottom (m)
- ν = kinematic viscosity of jet fluid (m^2/s)

Equation 2 can be rearranged to express the radius as a function of the jet parameters and the applied stress, and the applied stress can be equated to the critical stress for erosion of the bed at the experimentally measured ECR of each test condition. A least squares regression is used to fit the measured ECR to equation 2 where the fit is optimized by adjusting τ_w, thus approximating the critical stress required to erode the bed as the wall stress. The rate of erosion is not considered in this approach, so this analysis does not consider whether the estimated critical stress is for surface or mass erosion or complete failure (e.g. see Wells et al. 2009).

As described in *Summary of Pulse Jet Testing for Newtonian, Non-Newtonian Beds and Jets*, different test configurations were used. The data considered here includes the "full" beds wherein the fluid jets impinged into a previously undisturbed sediment bed as well as the "partial" beds wherein a fluid jet is impinged into a sediment bed that has been previously been eroded by a lower velocity jet

.

In Figure 5, the data and data fits are shown for combination of the full and partial bed test data. Good agreement is achieved between the Poreh et al. (1967) model and the measured data when a single value of critical stress is applied to the respective data sets. The estimated critical stress values are listed in the legend.

Increasing critical stress is estimated for the Newtonian and non-Newtonian interstitial fluid beds when eroded by the Newtonian fluid (NB-NJ and NNB-NJ), and a higher critical stress is estimated for the non-Newtonian fluid erosion of the non-Newtonian interstitial fluid bed (NNB:NNJ). This same relation is observed for only the "partial bed" data sets as shown in Figure 6, and there is minimal differences the estimated critical stress between the entire and partial bed data sets. A full bed data set is not evaluated given the lack of multiple velocity data points. Difference in ECR due to difference in the fluid or difference in the bed is considered.

As summarized in Wells et al. (2009), the resistance of a cohesive material (i.e. non-Newtonian yield stress fluid) to erosion depends on the strength of the cohesive forces binding the particles. Cohesion may far outweigh the influence of the physical characteristics of the individual particles. A heterogeneous bed comprised of noncohesive particles with cohesive interstitial fluid may have an increased critical stress for erosion in comparison to a bed of the same noncohesive particles with noncohesive interstitial fluid depending on the relation of the cohesive, adhesive, and frictional forces. The increase in estimated critical stress from the NB-NJ to NNB-NJ tests suggests that, for the test materials considered here with constant volume fraction of the glass particles, the cohesive property of the interstitial fluid increases the required stress.

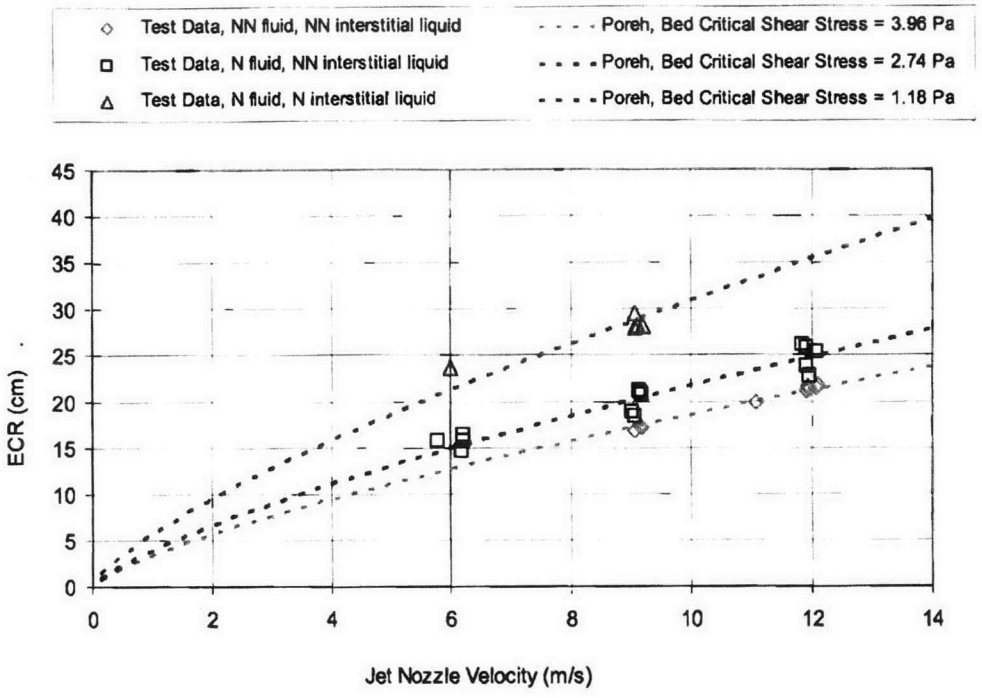

Figure 6 ECR as a Function of Fluid Jet Nozzle Velocity, partial bed data set

From Figure 5 and Figure 6, note that the jet nozzle velocity required to achieve equivalent measured ECRs of approximately 25 cm for the NB-NJ and NNB-NJ tests was approximately 6 and 12 m/s respectively, or nominally a factor of two increase for the non-Newtonian bed. This factor of increase in Newtonian jet velocity for equivalent measured ECRs between the two different beds is in reasonable agreement with that predicted from the thin cohesive layer ECR models of Gauglitz et al. (2009) written for equivalent ECR for different bed shear strengths as

$$\frac{U_{\tau_{S,NN}}}{U_{\tau_{S,N}}} = \left(\frac{\tau_{S,NN}}{\tau_{S,N}}\right)^{\frac{1}{2}} \qquad \text{Equation 3}$$

where $\tau_{S,NN}$ and $\tau_{S,N}$ are the shear strengths of the Newtonian and non-Newtonian beds, respectively. Using Eq. (3) with the bed strengths as 3197 and 573 Pa respectively (average shear strength of the vortexed samples under supernate (project document 24590-RMCD-03354), a velocity ratio of ~2.4 is achieved. Although the relation of a shear vane measurement of a granular non-cohesive bed to an intrinsic material property is subject to uncertainty (Daniels et al. 2007), the relative agreement of the experimental and predicted difference in bed erosion for the NB-NJ and NNB-NJ tests provides strong indication that the Newtonian and non-Newtonian beds erode differently.

This difference in erosion for the Newtonian and non-Newtonian beds is further considered by comparing the estimated increase in critical stress (see Figure 5 and Figure 6) to calculated critical stresses for the

Newtonian and non-Newtonian beds as summarized in Table 1. The calculated critical stresses are determined from empirical models that are dependent on other measured or estimated bed properties. The Brownlie (1981) expression for the Shields diagram is used for the critical stress of the Newtonian interstitial fluid bed. This expression is useful for non-cohesive solids, which are represented on the Shields diagram with the shear Reynolds numbers greater than approximately 2 (Wells et al. 2011). Estimates for the critical stress of the non-Newtonian interstitial fluid bed are made using the models listed in Table 1.

Table 1 Comparison of Critical Stress for Erosion for Test Conditions

Test Condition	Critical Stress for Erosion (Pa)	
	Data Fit	Model (reference)
NB-NJ	1.07	0.79 (Brownlie 1981) 0.98 (Cao et al 2006)
NNB-NJ	2.73	0.995 (Kothyari and Jain 2008) 3.09 (Wells et al. 2009)[1] 9.43 (Onishi et al. 2010)[1,2] 0.07 (Clark and Wynn 2007)[1] 0.71 (Clark and Wynn 2007)[3] 0.99 (Torfs et al. 2001)[4] 0.83 (Righetti and Lucarelli 2007)[4]
NNB-NNJ	3.97	N/A

1. Plasticity Index of 34 for kaolin clay (Wells et al. 2010) assumed for bed.
2. Clay slurry Bingham yield stress of 14 Pa used for bed shear strength.
3. Volume weighted median particle size of glass beads and clay.
4. Determined as described in 24590-WTP-RPT-ENG-11-001, Rev 0.

Caution must be taken in applying the critical stress for erosion relations for a given particulate or bed directly to a different material. Wells et al. (2009) noted that there does not appear to be tools for predicting sediment erosion without obtaining data for similar or related types of material. Clark and Wynn (2007) compared different methods of determining the critical shear stress for erosion. Jet erosion test results were compared to estimates from the Shields' diagram and empirical relations based on parameters of percent clay, plasticity index, particle size, and percent silt-clay. The jet erosion test results were as much as four orders of magnitude greater than the Shields diagram and empirical methods for cohesive materials indicating that models applied outside of the specific study area should be applied with caution.

The NN bed calculated critical stress are typically larger than that for the Newtonian bed, Table 1, but range by three orders of magnitude. Clearly, even accounting for the uncertainty of the input parameters, these results demonstrate the concerns of the previous paragraph, and limited comparison can be made to the fitted critical stress results.

The increase in the data fit critical stress for the NNB-NNJ in comparison with the NNB-NJ shown in Table 1 may be caused by the non-Newtonian jet overcoming the non-Newtonian supernatant fluid as well as the non-Newtonian interstitial fluid bed. Thus, the apparent critical stress of the non-Newtonian interstitial fluid bed is increased as estimated by the Poreh jet decay equation (Eq. (2)).

The difference in the experimentally measured ECR due to difference in the fluid and bed has been considered. The evaluations all indicate that the critical stress for erosion of the Newtonian and non-Newtonian interstitial fluid beds are different, and likely cause differences in the measured ECRs. The

increase in estimated critical stress for the NNB-NNJ test over the NNB-NJ tests may suggest there is a difference in the Newtonian and non-Newtonian fluid jets.

4.5 Assessment of Test 5 Scoping Study Parameters

4.5.1 Newtonian-Flow Clearing of the Non-Cohesive Bed

A prediction made prior testing for the critical shear stress for mobilization of the noncohesive glycerol/glass beads bed by an impinging Newtonian glycerol jet using the Brownlie (1981) form of the Shields relation is $\tau_c = 0.79$ Pa. The normalized difference between this prediction and the observed value of 1.07 Pa is (1.07-0.79)/0.79=0.35 or 35% of the predicted value. A similar prediction using the Cao et al. (2006) form of the Shields relation is $\tau_c = 0.98$ Pa. Its normalized difference is (1.07-0.98)/0.98 = 0.09 or 9% of the predicted value.

Figure 7, extracted from Miller, McCave, and Komor (1977), shows the original Shields data. The gray band provides a visual indication of the data scatter. At the conditions of the Test 5 Scoping Study Newtonian tests, the data scatter is approximately 33% of the central value.[1] Values for the Shields parameter[2] from the Brownlie (1981) and Cao et al. (2006) models are approximately 0.06 and 0.07, respectively. They have been added to this figure. The Brownlie (1981) prediction is consistent with the central value of the Shields parameter based on the original Shields data. The Cao et al. (2006) prediction lies at the upper end of this range. Miller et al. (1977) extended the dataset contributing to the Shields relation (see Figure 8). The Shields parameters for the Brownlie (1981) and Cao et al. (2006) predictions have been added to this figure. The central value is near 0.07. The data scatter is bounded by 0.04 and 0.1, a band that is approximately (0.1-0.04)/0.07 = 0.86 or 86% of the central value. The Cao et al. (2006) prediction represents the central value of Figure 8 better than the Brownlie (1981) relation. For purposes of analysis, use of the Cao et al. (2006) model with an effective half width for data scatter of ±43% is recommended.

[1] This estimate was made by calculating the shear Reynolds number, $Re_* = u_* d_p/\nu_l$, using $\nu_l = 9.4\text{x}10\text{-}6$ m^2/s, ρ_l = 1158 kg/m^3, and d_p = 775 μm, where $u_* = (\tau_c/\rho_l)^{0.5}$ for both predictions. The calculated values for Re_* are both near 2, 2.2 for the Brownlie (1981) expression and 2.4 for Cao et al. (2006) expression. The range for the Shields parameter ($\theta_f = \tau_w/(\rho_l s_p g d_p)$, ordinate of Fig. 1) was extracted visually (0.05 to 0.07) for $Re_* = 2$. The central value is $\theta_f = 0.06$. The difference compared to the central value is (0.07-0.05)/0.06 = 0.33 or 33%.

[2] Using $\rho_p = 2900$ kg/m^3, $s_p = (\rho_p - \rho_l)/\rho_l = 1.5$, and $g = 9.81$ m/s^2

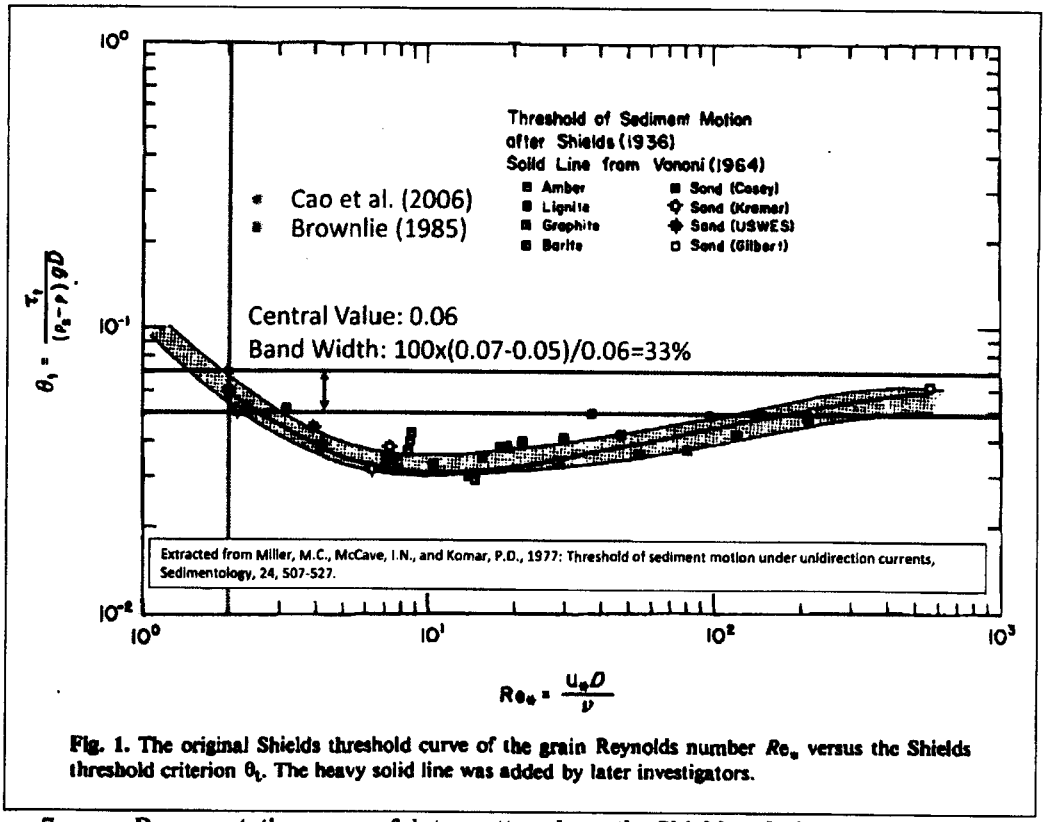

Fig. 1. The original Shields threshold curve of the grain Reynolds number Re_* versus the Shields threshold criterion θ_t. The heavy solid line was added by later investigators.

Figure 7 **Representative range of data scatter about the Shields relations based on Shields original dataset.**

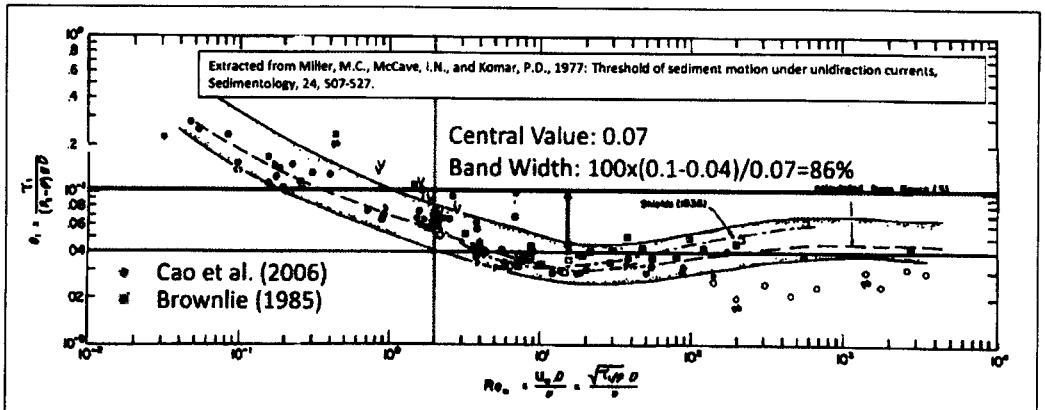

Fig. 2. The proposed modified Shields curve of θ_t versus Re_* based on additional carefully selected data. See Table 1 for identification of the symbols.

Figure 8 **Representative range of data scatter about the Shields relations based on an expanded dataset.**

4.5.2 Non-Newtonian Clearing of the Cohesive Bed

A prediction made prior testing for the critical shear stress for mobilization of the cohesive slurry/glass beads bed by an impinging non-Newtonian clay slurry using the Cao et al. (2006) form of the Shields relations augmented by the Kothyari and Jain (2008)correlation for a silt-sand bed is τ_{cc} = 1.27 Pa. The normalized difference between the prediction and the observed value of 3.97 Pa is (3.97-1.27)/1.27 = 2.13 or 213% of the predicted value.

The range for data scatter about the estimate of τ_{cc} is estimated by compounding the data scatter bounds for the Cao et al. (2006) form of the Shields relation for τ_c and for the Kothyari and Jain (2008) correlation for the ratio τ_{cc}/τ_c. Using ±43% as the range for data scatter about the Shields relation and ±50% (see Figure 9) as a representative range for data scatter about the Kothyari and Jain (2008) correlation (see Figure 9), the estimated range for data scatter about τ_{cc} is (1 ± 0.43) x (1 ± 0.50) – 1 = ±1.145 or ±114.5%. The observed difference is approximately twice this value. Figure 9 shows one value lying outside of the +50% bound. It is contained within the +100% bound. Using this value to assess the plausible range for data scatter about τ_{cc} yields (1 ± 0.43) x (1 ± 1.00) – 1 = ±1.86 or ±186%. The observed difference of 213% is still greater than this value. The data indicate that either the Kothyari and Jain (2008) model is not valid for estimating the critical shear stress for mobilization of the cohesive bed used in the Test 5 Scoping Study or that the bed parameters used in the Kothyari and Jain (2008) model were not properly characterized.

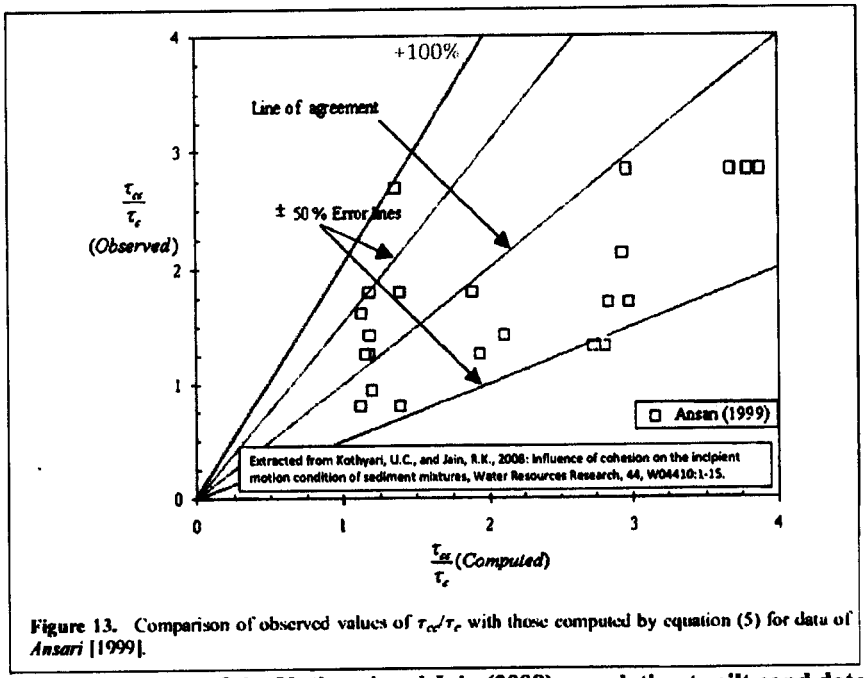

Figure 13. Comparison of observed values of τ_{cc}/τ_c with those computed by equation (5) for data of *Ansari* [1999].

Figure 9 Fit of the Kothyari and Jain (2008) correlation to silt-sand data.

4.5.3 Post-Test Characterization of the Input Parameters to Kothyari and Jain (2008) Silt-Sand Relation for The Test 5 Scoping Study

The Kothyari and Jain (2008) silt-sand correlation for the ratio of the critical shear stress to mobilize a cohesive bed relative to the Shields prediction for the critical shear stress to mobilize a similar bed without cohesion is

$$\frac{\tau_{cc}}{\tau_c} = 1.88\left(1+P_c\right)^{3/2} e^{-1/6}\left(1+0.001UCS^*\right)^{9/20} - 1.0$$

Equation 4

It depends on three parameters: the weight fraction of the fine-grain sediment in the solids bed, P_c, the void ratio (liquid to solids volume fraction ratio), e, and the unconfined compressive strength of the bed, UCS.

By intent, the Test 5 Scoping Study cohesive bed material was formed to be 60% glass beads and 40% clay slurry (27% bentonite-bentonite[3] clay to 73% salt water[4] composition by weight). This ratio was meant to represent a settled solids bed with random arrangement with clay slurry filling the interstitial space. The Test 5 Scoping Study bed was constructed by screeding the bed material to a thickness of 0.25 inches on the box flume floor. An observation during processing of the bed material is that some separation of fluid from the solids occurred.

Figure 10 shows a free standing cylinder of the Test 5 Scoping Study bed material (note this cylinder is deeper than the 1/4" bed). The image shows that the material supports load and that fluid leakage from the material occurs, as was observed during screeding of the Test 5 Scoping Study bed. The image also shows considerable organization of the glass beads[5]. Both organization of the glass beads in the bed material and fluid leakage would affect an estimate of the bed stress using the silt-sand correlation from Kothyari and Jain (2008). The observed glass bead organization implies that the achieved packing factor in the screeded Test 5 Scoping Study bed exceeded the 60% target. A greater density of glass beads would lead to a decrease in the clay faction of the bed, a decrease in the void ratio, and possibly an increase in the unconfined compressive strength of the bed.[6]

The packing limit of closely packed spheres, 74%, might be used as a conservative upper value for the model packing factor of the packed Test 5 Scoping Study bed.

[3] Clay composition: 80% Kaolin with 20% Bentonite by weight
[4] Salt water composition: 99.863% Richland water with 0.137% NaCl by weight
[5] Packing factor thresholds for spheres: random packing (up to 64%), close packing (74%), maximum packing (approximately 78%) (source http://mathworld.wolfram.com/SpherePacking.html)
[6] In a private communication, Jim Huckaby of The Pacific Northwest National Laboratories (PNNL) said that he believed that the volume fraction of the glass beads was greater than 60% but not much greater than 63%.

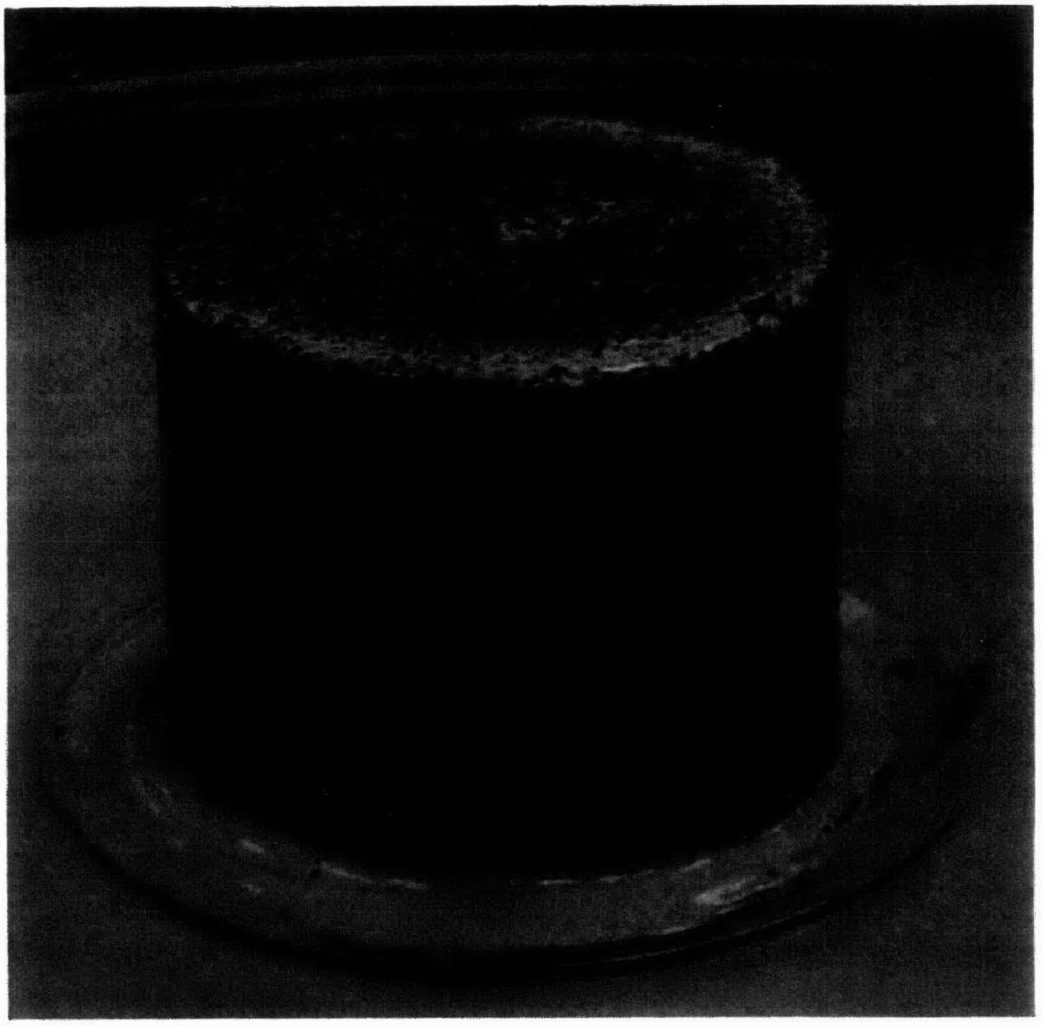

Figure 10 **Free standing cylinder of Test 5 Scoping Study bed material demonstrating an ability to support load and showing significant organization of the glass beads and liquid leakage.**

No data was collected to know whether the leaked fluid from the Test 5 Scoping Study bed material was clay slurry or was predominantly liquid. If the fluid was predominantly liquid and not clay, there would be an increase in the bed material clay content over the liquid content and a corresponding decrease in the bed void ratio. Based on available data, no suggestions for conservative bounds for the clay fraction by weight, Pc, or the bed void ratio, e, can be made.

Also, no data was identified prior to testing which would hint at an expectation for *UCS*. Pretest estimates used the proposal from project document, 24590-QL-HC9-WA49-00001-03-00025 (WTP-RPT-177), page B-13, which reports that *UCS* for a material might be estimated as twice the material's shear strength. Based on this relation, project document 24590-WTP-RPT-ENG-11-001, Rev 0, "*Determination that Non-Newtonian Vessels Can Be Evaluated Using Newtonian Techniques*", proposes that *UCS* might

be modeled as twice the Bingham fluid yield stress, τ_0, for a naturally settled, unpacked, coarse-grain sediment bed which might be expected to retain much of the character of the clay slurry. Based on Hanford data, Onishi et al. (2011) suggests use of 2.3 rather than 2.0 for the model constant. The measured yield stress for the Test 5 Scoping Study slurry is reported to be approximately 13.6 Pa (see project document 24590-RMCD-03354). If the *UCS* model proposed in project document 24590-WTP-RPT-ENG-11-001, were to be valid for the packed cohesive, clay slurry/glass beads bed of the Test 5 Scoping Study, the estimated yields stress for that bed would be approximately 2.3 x 13.6 Pa = 31.3 Pa (the pretest prediction was 27.2 Pa using 2 as the model constant). Shear strength measurements for the Test 5 Scoping Study bed material are reported in project document 24590-RMCD-03354. They range from a low value near 1000 Pa to a high value greater than 3938 Pa and imply that UCS is expected to lie within a range from 2.3 x 1000 Pa = 2300 Pa to an upper value greater than 2.3 x 3938 Pa = 9057 Pa. These values are two orders of magnitude greater than the 31.3 Pa pretest prediction showing that *UCS* is not directly related to τ_0 in a way that is understood and that the model proposed in project document 24590-WTP-RPT-ENG-11-001 is not valid for the packed cohesive bed used in the Test 5 Scoping Study.

Estimation of the critical shear stress for mobilization of the cohesive Test 5 Scoping Study bed with the Kothyari and Jain (2008) silt-sand model using an upper bound for the bed packing factor of 74%, an interstitial fluid composition equal to the composition of the clay slurry, and *UCS* = 2300 Pa yields a prediction for τ_{co}/τ_c of 1.61:

Calculate P_c:

$$wt\%_{beads}(bed) = \frac{100\,wt\% \cdot \rho_{beads} Vol\%_{beads}}{\left(\rho_{beads} Vol\%_{beads} + \rho_{slurry} Vol\%_{slurry}\right)} = \frac{100\,wt\% \cdot 2900 \cdot 74}{\left(2900 \cdot 74 + 1200 \cdot 26\right)} = 87.31\,wt\%$$

$$wt\%_{slurry}(bed) = 100\,wt\% - wt\%_{beads}(bed) = 100\,wt\% - 87.31\,wt\% = 12.69\,wt\%$$

$$wt\%_{clay}(bed) = \frac{wt\%_{clay}(slurry)}{100} wt\%_{slurry}(bed) = \frac{27}{100} 12.69\,wt\% = 3.43\,wt\%$$

$$P_c = \frac{wt\%_{clay}(bed)}{100} = \frac{3.43\,wt\%}{100} = 0.0343$$

Calculate e:

$$Vol\%_{clay}(bed) = \frac{Vol\%_{clay}(slurry)}{100} Vol\%_{slurry}(bed) = \frac{12.29}{100} 26.00\,Vol\% = 3.20\,Vol\%$$

$$Vol\%_{salt-water}(bed) = 26.00\,Vol\%_{slurry}(bed) - 3.20\,Vol\%_{clay}(bed) = 22.80\,Vol\%$$

$$e = \frac{Vol\%_{salt-water}(bed)}{Vol\%_{beads}(bed) + Vol\%_{clay}(bed)} = \frac{22.80}{74.00 + 3.20} = 0.2954$$

Calculate d_a:

$$d_a = \frac{wt\%_{beads}(\text{bed})\, d_{beads} + wt\%_{clay}(\text{bed})\, d_{clay}}{wt\%_{beads}(\text{bed}) + wt\%_{clay}(\text{bed})} = \frac{87.31 \cdot 775\,\mu m + 3.43 \cdot 5.597\,\mu m}{87.31 + 3.43} = 746\,\mu m$$

Calculate UCS^*:

$$UCS^* = \frac{UCS}{\rho_f s_a g d_a} \approx \frac{2300\,Pa}{\rho_f s_a g d_a} = \frac{2300}{1200 \cdot 1.417 \cdot 9.81 \cdot 7.46\text{x}10^{-4}} = 184.89$$

Calculate τ_{cc}/τ_c:

$$\frac{\tau_{cc}}{\tau_c} = 1.88\left(1+P_c\right)^{3/2} e^{-1/6}\left(1+0.001UCS^*\right)^{9/20} - 1.0$$
$$= 1.88\left(1+0.0343\right)^{3/2} 0.2954^{-1/6}\left(1+0.001 \cdot 184.89\right)^{9/20} - 1.0$$
$$= 1.615$$

The observed ratio of τ_{cc}/τ_c is 3.96 Pa/1.07 Pa = 3.36. The observed value is greater than the predicted value by a factor of 2.08 which places the prediction at the +100% boundary for the Kothyari and Jain (2008) relation and thus is plausible relative to the extreme values in the observed data scatter. The prediction for τ_{cc}/τ_c increases to 2.1, if UCS = 9057 Pa, is used:

Calculate UCS^*:

$$UCS^* = \frac{UCS}{\rho_f s_a g d_a} \approx \frac{9057\,Pa}{\rho_f s_a g d_a} = \frac{9057}{1200 \cdot 1.417 \cdot 9.81 \cdot 7.46\text{x}10^{-4}} = 728.06$$

Calculate τ_{cc}/τ_c:

$$\frac{\tau_{cc}}{\tau_c} = 1.88\left(1+P_c\right)^{3/2} e^{-1/6}\left(1+0.001UCS^*\right)^{9/20} - 1.0$$
$$= 1.88\left(1+0.0343\right)^{3/2} 0.2954^{-1/6}\left(1+0.001 \cdot 728.06\right)^{9/20} - 1.0$$
$$= 2.099$$

The observed value for τ_{cc}/τ_c is greater than this prediction by a factor of 1.7. Were one able to account for increased clay content and reduced fluid content in the handled Test 5 Scoping Study bed material, a further reduction in the ratio of the observed value for τ_{cc}/τ_c relative to the predicted one could be reported.

4.6 Summary

A comparison of pre-test predictions for the Test 5 Scoping Study to post-test data demonstrate that the Cao et al. (2006) model correlates that range of Shields data better than the Brownlie model for estimating the critical shear stress to mobilize a non-cohesive settled solids bed. Similar comparisons of pre-test predictions to post-test data do not appear to support use of the Kothyari and Jain (2008) silt-sand relation for estimating the critical shear stress to mobilize a packed bed of cohesive settled solids. The post-test analysis, however, strongly supports the conclusion that the Test 5 Scoping Study bed parameters were not properly characterized. Recalculation of the Kothyari and Jain (2008) predictions for τ_{cc}/τ_c based on post-test characterization of the Test 5 Scoping Study bed material yields the different conclusion that the Kothyari and Jain (2008) silt-sand model for the critical shear stress to mobilize a cohesive settled solids bed may indeed be valid for use in computing τ_{cc} for the Test 5 Scoping Study bed material.

Post-test analysis leads to the conclusion that the Test 5 Scoping Study results are inadequate to confirm whether or not the engineering approximation that "a sheared Bingham fluid under conditions

representative of WTP PJM vessels achieves a Newtonian-like state during drive both in the bulk flow of the activated bottom region of a WTP PJM vessel and near the bottom boundary" is valid.

5 Possible Candidates for Additional Investigations

The analyses of the test data indicate that there are differences in the Newtonian and non-Newtonian interstitial fluid beds and their interactions with the Newtonian and non-Newtonian fluid jets that are not accounted for via corrections based on correlations for the critical stress for erosion of those beds. Thus, the use of the erosion or effective cleaning radius of these beds as a metric for evaluating the similarity or difference of the jet-mixing performance of the Newtonian and non-Newtonian fluid jets has not been successful. Alternate metrics to evaluate the jet-mixing performance of the Newtonian and non-Newtonian fluid jets that are not confounded in a similar manner are suggested. These options include visual observation of the region-of influence of the fluid jet into a synonymous fluid and direct measurement of the applied stress of the fluid jets.

Visual observation would use a tracer die injected as part of the jet flow. Obvious limitations that would have be addressed in this approach include the opacity of the non-Newtonian clay slurry as well as the rapid mixing of the Newtonian liquid. These issues would likely be exacerbated in a multi-jet system, thereby limiting the ability to understand jet-to-jet interactions.
Direct measurement of the applied stress of a fluid jet as a function of radii is subject to the limitations of the applied sensor. Providing that potential limitations can be addressed, the ability to understand jet-to-jet interactions may still be limited. However, the direct measurement of the wall stress will likely most readily provide the most conclusive data for the similarity or difference of the jet-mixing performance of the Newtonian and non-Newtonian fluid jet.

If testing is continued with the box flume, it would be useful to perform fluid-only tests where shear on the box-flume floor is directly measured and where the jet material is dyed to allow a direct visual assessment of the fluid penetration footprint.

If testing is continued with the box flume using a solids bed, an approach needs to be devised to form the bed through natural settling, not through screeding a premixed material, to better represent conditions in WTP PJM vessels.

Vessel testing might be the better approach. The 8 Ft vessel is a candidate. Advantages are the ability to form a settled solids bed, as it would form at the plant, and to have a sheared upper region via sparging, as occurs in the plant. We can note that Test 3 to Test 7 comparisons (not included) clearly suggest that vessel conditions are different from the Test 5 Scoping Study conditions.

For all tests using a settled solids bed, explicit measurements of the bed characteristics are needed to pin down the parameters in the Kothyari and Jain (2008) model in order to understand the extent to which their correlation is valid at the WTP. Preliminary analysis suggests that their model might be valid, if the bed parameters are well characterized.

6 Conclusions

Test 5 Scoping Study data indicate that there is sufficient uncertainty in the fluid (turbulence) and bed (uncertain characterization) conditions to preclude an assessment of whether a sufficiently sheared

Bingham fluid may be analyzed using Newtonian flow assumptions. The current test data are insufficient and the Test 5 design of experiment may be inadequate. Because extensive additional testing and development of new measurement and analysis techniques might be required to yield a successful Test 5 experiment, with no clear route to success, it was decided that, Newtonian techniques will not be used to assess non-Newtonian vessel performance and that project document 24590-WTP-RPT-ENG-11-001, Rev 0. 2011, *Determination that Non-Newtonian Vessels Can Be Evaluated Using Newtonian Techniques*, which provided the basis for the assumption, will be cancelled.

7 References

24590-QL-HC9-WA49-00001-03-00025, Rev A, 2009, *An Approach to Understanding Cohesive Slurry Settling, Mobilization, and Hydrogen Gas Retention in Pulsed Jet Mixed Vessels* (WTP-RPT-177).

24590-WTP-RPT-ENG-11-001, Rev 0. 2011, *Determination that Non-Newtonian Vessels Can Be Evaluated Using Newtonian Techniques.*

24590-RMCD-03354, 2011, *Summary of LSIT-Info-N-NN-ECR-005 & 5a, Phase I: Single PJM, Determination If Non-Newtonian Vessels Can Be Evaluated Using Newtonian Techniques Using 0.25-In. Bed Depth.*

CCN 238153, memorandum, R Hanson (WTP) to R Daniel (WTP), *Testing Associated With the Determination that Non-Newtonian Vessels can be Evaluated Using Newtonian Techniques*, 18 October 2011.

Brownlie WR. 1981. *Prediction of Flow Depth and Sediment Discharge in Open Channels.* Rep. KH-R-43A, California Institute of Technology, Pasadena, California.

Cao, Z., Pender, G., and Meng, J., 2006: *Explicit formulation of the Shields diagram for incipient motion of sediment*, J. Hydr. Eng., Oct., 1097-1099.

Clark LA, and TM Wynn. 2007. Methods for Determining Streambank Critical Shear Stress and Soil Erodibility: Implications for Erosion Rate Predictions. *Transactions of the American Society of Agricultural Engineers.* 50(1):95-106.

Daniel RC, AP Poloski, and AE Saez. 2007. Vane Rheology of Cohesionless Glass Beads. *Powder Technology.* 181 (2008) 237 - 248.

Gauglitz PA, BE Wells, JA Fort, PA Meyer. 2009. *An Approach to Understanding Cohesive Slurry Settling, Mobilization, and Hydrogen Gas Retention in Pulsed Jet Mixed Vessels.* PNNL-17707, WTP-RPT-177, Rev. 0. Pacific Northwest National Laboratory, Richland, WA (24590-QL-HC9-WA49-00001-03-00025).

Kothyari UC, and RK Jain. 2008. Influence of cohesion on the incipient motion condition of sediment mixtures. *Water Resources Research*, Volume 44, W04410:1-15.

Miller, M.C., McCave, I.N., and Komar, P.D., 1977: *Threshold of sediment motion under unidirection currents*, Sedimentology, 24, 507-527.

Onishi Y., Baer, E.B.K., Chun, J., Sande, S.A., Yokuda, S.T., Schmidt, A.J., Enderlin, C.W., Buchmiller, W.C., Riley, B.J., and Crum, J.V., 2011: *Development of K-Basin High-Strength Homogeneous Sludge Simulants and Correlations Between Unconfined Compressive Strength and Shear Strength.* PNNL-20048 Rev. 1 (53451-RPT14 Rev 1). Pacific Northwest National Laboratory, Richland, WA.

Onishi Y, ST Yokuda, and AJ Schmidt. 2010. *Evaluation of Shear Strength Threshold of Concern for Retrieval of Interim-Stored K-Basin Sludge in the Hanford Site.* PNNL-19946. Pacific Northwest National Laboratory, Richland, WA.

Poreh M, YG Tsuei, and JE Cermak. 1967. "Investigation of a Turbulent Radial Wall Jet." *Journal of Applied Mechanics*, June 1967, 457 - 463.

Righetti M, and C Lucarelli. 2007. May the Shields Theory Be Extended to Cohesive and Adhesive Benthic Sediments?, *J. Geophys. Res.*, 112, C05039:1-14.

Torfs H, J Jiang, and AJ Mehta. 2001. Assessment of Erodibility of Fine/Coarse Sediment Mixtures. *Coastal and Estuarine Fine Sediment Processes*. Elsevier Science B.V., WH McAnally and AJ Mehta, editors.

Wells BE, PA Gauglitz, and DR Rector. 2011. *Comparison of Waste Feed Delivery Small Scale Mixing Demonstration Simulant to Hanford Waste.* PNNL-20637. Pacific Northwest National Laboratory, Richland, WA.

Wells BE. JJ Jenks, G Boeringa, NN Bauman, and AD Guzman. 2010. *Lateral Earth Pressure at Rest and Shear Modulus Measurements on Hanford Sludge Simulants.* PNNL-19829. Pacific Northwest National Laboratory, Richland, WA.

Wells BE, CW Enderlin, PA Gauglitz, and RA Peterson. 2009. *Assessment of Jet Erosion for Potential Post-Retrieval K-Basin Settled Sludge.* PNNL-18831. Pacific Northwest National Laboratory, Richland, WA.

Appendix A
Test 5 Scoping Study Carrier Fluid and Bed Parameters

A.1 Newtonian Fluid Parameters

The Newtonian flow test conditions are outlined in project document 24590-RMCD-03354, *Summary of LSIT-Info-N-NN-ECR-005 & 5a, Phase I: Single PJM, Determination If Non-Newtonian Vessels Can Be Evaluated Using Newtonian Techniques Using 0.25-In. Bed Depth.*

The carrier fluid for the Newtonian flow tests was glycerol with 37 wt% water to 63 wt% glycerin composition. At room temperature, water and glycerin densities are $\rho_{water} = 998$ kg/m^3 and $\rho_{glycerin} = 1260$ kg/m^3. The glycerol density at room temperature is calculated from the volume relation $Vol_{glycerol} = Vol_{water} + Vol_{glycerin}$ using $Vol_{glycerol} = Mass_{glycerol}/\rho_{glycerol}$, $Vol_{water} = Mass_{water}/\rho_{water}$, and $Vol_{glycerin} = Mass_{glycerin}/\rho_{glycerin}$. Substitution and reorganization yields

$$\rho_{glycerol} = \frac{1}{\frac{wt\%_{water}}{100}\frac{1}{\rho_{water}} + \frac{wt\%_{glycerin}}{100}\frac{1}{\rho_{glycerin}}} = \frac{1}{\frac{0.37}{998\,kg/m^3} + \frac{0.63}{1260\,kg/m^3}} = 1148\frac{kg}{m^3}$$

Here $wt\%_{water} = 100 \times Mass_{water}/Mass_{Total}$ and $wt\%_{glycerin} = 100 \times Mass_{glycerin}/Mass_{Total}$. The average of as-measured values for the density and viscosity of the Test 5 Scoping Study glycerol solution are $\rho_{glycerol} = 1158$ kg/m^3 and $\mu_{glycerol} = 10.88$ cP, respectively.

A.2 Non-Newtonian Fluid Parameters

The non-Newtonian flow test conditions are outlined in project document 24590-RMCD-03354, *Summary of LSIT-Info-N-NN-ECR-005 & 5a, Phase I: Single PJM, Determination If Non-Newtonian Vessels Can Be Evaluated Using Newtonian Techniques Using 0.25-In. Bed Depth.*

The composition of the non-Newtonian slurry used in Test 5 Scoping Study was 21.6 wt% kaolin clay ($\rho_{kaolin} = 2600$ kg/m^3), 5.4 wt% bentonite clay ($\rho_{bentonite} = 2795$ kg/m^3), 0.1 wt% NaCl ($\rho_{NaCl} = 2165$ kg/m^3), and 72.9 wt% water ($\rho_{water} = 998$ kg/m^3) yielding a slurry density, ρ_{slurry}, of

$$\rho_{slurry} = \frac{1}{\frac{wt\%_{kaolin}}{100}\frac{1}{\rho_{kaolin}} + \frac{wt\%_{bentonite}}{100}\frac{1}{\rho_{bentonite}} + \frac{wt\%_{NaCl}}{100}\frac{1}{\rho_{NaCl}} + \frac{wt\%_{water}}{100}\frac{1}{\rho_{water}}}$$

$$= \frac{1}{\frac{0.216}{2600\,kg/m^3} + \frac{0.054}{2795\,kg/m^3} + \frac{0.001}{2165\,kg/m^3} + \frac{0.729}{998\,kg/m^3}}$$

$$= 1200\frac{kg}{m^3}$$

The slurry rheology is approximated using a Bingham-fluid model. The average of as-measured values for the Bingham fluid consistency and Bingham fluid yield stress of the Test 5 Scoping Study slurry are $\mu_{\infty,Slurry}$ = 11.3 cP and $\tau_{0,Slurry}$ = 13.6 Pa, respectively.

A.3 Non-Cohesive Bed Parameters

The non-cohesive bed parameters are outlined in project document 24590-RMCD-03354, *Summary of LSIT-Info-N-NN-ECR-005 & 5a, Phase I: Single PJM, Determination If Non-Newtonian Vessels Can Be Evaluated Using Newtonian Techniques Using 0.25-In. Bed Depth.*

Non-cohesive packed beds in Test 5 Scoping Study are formed by mixing 775 μm glass beads (ρ_{beads} = 2900 kg/m^3) with the glycerol carrier fluid in a proportion to yield a glass beads packing factor of 0.6. The critical shear stress for mobilization of this bed by the glycerol carrier fluid, τ_c, is estimated using the Shields relations as expressed by Brownlie (1981) and by Cao et al. (2006).

Parameters required for estimating τ_c for the non-cohesive glass-beads/glycerol beds in Test 5 Scoping Study are

- the carrier fluid density, $\rho_f = \rho_{glycerol}$ = 1158 kg/m^3,
- the carrier fluid dynamic viscosity, $\mu_f = \mu_{glycerol}$ = 10.88 cP = 0.01088 kg/(m s),
- the carrier fluid kinematic viscosity, $\nu_f = \nu_{glycerol}$ = 0.01088/1158 m^2/s = 9.396x10^{-6} m^2/s,
- the submerged specific gravity with respect to the carrier fluid based on the bed-averaged particle density, $s_a = (\rho_{beads} - \rho_f)/\rho_f$ = (2900 kg/m^3 – 1158 kg/m^3)/1158 kg/m^3 = 1.50,
- the characteristic particle diameter for the solids in the packed bed based on the bed-averaged particle diameter, $d_a = d_{beads}$ = 775 μm = 7.75x10^{-4} m, and
- the acceleration of gravity, g = 9.81 m/s^2.

A.4 Brownlie (1981)

Brownlie (1981) proposes use of

$$\theta_c = \frac{\tau_c}{\rho_f s_a g d_a} = 0.22 d^{*-0.9} + 0.06 \exp\left(-17.73 d^{*-0.9}\right)$$

where d^* is the dimensionless length scale

$$d^* = \left(\frac{s_a g}{\nu_f^2}\right)^{1/3} d_a$$

θ_c is the critical value of the Shields parameter. The estimate for τ_c is computed using

$$\tau_c = \rho_f s_a g d_a \theta_c$$

For the non-cohesive glass-beads/glycerol beds in Test 5 Scoping Study,

$$d^* = \left(\frac{s_a g}{\nu_f^2}\right)^{1/3} d_a = \left(\frac{1.5 \cdot 9.81}{\left(9.396\text{x}10^{-6}\right)^2}\right)^{1/3} 7.75\text{x}10^{-4} = 4.269$$

and

$$d^{*-0.9} = 4.269^{-0.9} = 0.2708$$

The critical value for the Shields parameter is

$$\theta_c = 0.22 d^{*-0.9} + 0.06 \exp\left(-17.73 d^{*-0.9}\right) = 0.22 \cdot 0.2708 + 0.06 \exp\left(-17.73 \cdot 0.2708\right) = 0.0601$$

The Brownlie (1981) estimate for τ_c is

$$\tau_c = \rho_f s_a g d_a \theta_c = \left(1158 \cdot 1.50 \cdot 9.81 \cdot 7.75\text{x}10^{-4} \cdot 0.0601\right) \text{Pa} = 0.7956 \text{Pa}$$

A.5 Cao, Pender, and Meng (2006)

Cao et al. (2006) propose use of

$$\theta_c = \begin{cases} 0.1414 \text{Re}_p^{-0.2306}, & \text{Re}_p \le 6.61 \\ \dfrac{\left[1 + \left(0.0223 \text{Re}_p\right)^{2.8358}\right]^{0.3542}}{3.0946 \text{Re}_p^{0.6769}}, & \text{Re}_p \in (6.61, 282.84) \\ 0.045, & \text{Re}_p \ge 282.84 \end{cases}$$

where Re_p is a particle Reynolds number

$$\text{Re}_p = \frac{U_g d_a}{\nu_f}$$

U_g is a characteristic velocity for particle settling, $U_g = (s_a g d_a)^{1/2}$. For the non-cohesive glass-beads/glycerol beds in Test 5 Scoping Study,

$$U_g = \sqrt{s_a g d_a} = \sqrt{1.5 \cdot 9.81 \cdot 7.75\text{x}10^{-4}}\,\text{m/s} = 0.1069\,\text{m/s}$$

The particle Reynolds number is

$$\text{Re}_p = \frac{U_g d_a}{\nu_f} = \frac{0.1069 \cdot 7.75\text{x}10^{-4}}{9.396\text{x}10^{-6}} = 8.821$$

The critical value for the Shields parameter is

$$\theta_c = \frac{\left[1 + \left(0.0223\,\text{Re}_p\right)^{2.8358}\right]^{0.3542}}{3.0946\,\text{Re}_p^{0.6769}} = \frac{\left[1 + \left(0.0223 \cdot 8.821\right)^{2.8358}\right]^{0.3542}}{3.0946 \cdot 8.821^{0.6769}} = 0.0743$$

The Cao et al. (2006) estimate for τ_c is

$$\tau_c = \rho_f s_a g d_a \theta_c = \left(1158 \cdot 1.50 \cdot 9.81 \cdot 7.75\text{x}10^{-4} \cdot 0.0743\right)\text{Pa} = 0.9838\,\text{Pa}$$

A.6 Cohesive Bed Parameters

The cohesive bed parameters are outlined in project document 24590-RMCD-03354, *Summary of LSIT-Info-N-NN-ECR-005 & 5a, Phase I: Single PJM, Determination If Non-Newtonian Vessels Can Be Evaluated Using Newtonian Techniques Using 0.25-In. Bed Depth.*

Cohesive packed beds in Test 5 Scoping Study are formed by mixing 775 μm glass beads (ρ_{beads} = 2900 kg/m^3) with the clay slurry in a proportion to yield a glass beads packing factor of 0.6. The critical shear stress for mobilization of this bed by the clay slurry, τ_c, is estimated first by using the Shields relations as expressed by Brownlie (1981) and by Cao, et al. (2006) to estimate the critical shear stress for bed mobilization were the bed non-cohesive then by using the silt-sand correlation of Kothyari and Jain (2008) to inflate the non-cohesive bed estimate for the critical shear stress for bed mobilization to yield the cohesive bed estimate for the critical shear stress for bed mobilization.

The Kothyari and Jain (2008) silt-sand correlation for ratio of the critical shear stress for mobilization of a cohesive packed solids bed, τ_{cc}, to the critical shear stress for mobilization of the packed solids bed were it non-cohesive, τ_c, is

$$\frac{\tau_{cc}}{\tau_c} = 1.88\left(1 + P_c\right)^{3/2} e^{-1/6}\left(1 + 0.001 UCS^*\right)^{9/20} - 1.0$$

P_c is the percent fraction by weight of the fine-grain sediment in the solids bed; e is the void ratio (the liquid to solids volume fraction ratio) for the solids bed; and UCS^* is the non-dimensionalized unconfined compressive strength (UCS) for the bed material, $UCS^* = UCS/(\rho_f s_a g d_a)$.

By intent, the Test 5 Scoping Study cohesive bed material was formed to be 60% glass beads and 40% clay slurry by volume. The mass of glass beads in the packed bed is $Mass_{beads} = \rho_{beads}\ Vol_{bed}\ Vol\%_{beads}/100$. The mass of the clay slurry in the interstitial volume is $Mass_{slurry} = \rho_{slurry}\ Vol_{bed}\ Vol\%_{slurry}/100$. The total mass of the packed bed is $Mass_{bed} = Mass_{beads} + Mass_{slurry} = \rho_{beads}\ Vol_{bed}\ Vol\%_{beads}/100 + \rho_{slurry}\ Vol_{bed}\ Vol\%_{slurry}/100$. Using these relations, the glass beads fraction of the packed bed by weight is

$$wt\%_{beads}(bed) = 100\,wt\%\frac{Mass_{beads}}{Mass_{Total}} = 100\,wt\%\frac{\rho_{beads}Vol\%_{beads}}{\left(\rho_{beads}Vol\%_{beads} + \rho_{slurry}Vol\%_{slurry}\right)}$$

$$= 100\,wt\%\frac{2900\cdot 60}{\left(2900\cdot 60 + 1200\cdot 40\right)} = 78.38\,wt\%$$

The mass fraction of the interstitial volume of the packed bed by weight is

$$wt\%_{slurry}(bed) = 100\,wt\% - wt\%_{beads}(bed) = 100\,wt\% - 78.38\,wt\% = 21.62\,wt\%$$

The composition of the clay slurry is 21.6 wt% kaolin and 5.4 wt% bentonite for a total of 27 wt% clay yielding a clay fraction for the packed bed of

$$wt\%_{clay}(bed) = \frac{wt\%_{clay}(slurry)}{100}wt\%_{slurry}(bed) = \frac{27}{100}21.62\,wt\% = 5.84\,wt\%$$

The corresponding mass fraction of clay in the packed bed is then

$$P_c = \frac{wt\%_{clay}(bed)}{100} = \frac{5.84\,wt\%}{100} = 0.0584$$

The nominal particle size for the kaolin in the clay is 5.73 µm. The nominal particle size for the bentonite in the clay is 5.065 µm. The mass weighted average particle size in the clay, d_{clay}, is

$$d_{clay} = \frac{wt\%_{kaolin}(\text{clay})\,d_{kaolin} + wt\%_{bentonite}(\text{clay})\,d_{bentonite}}{wt\%_{kaolin}(\text{clay}) + wt\%_{bentonite}(\text{clay})}$$

$$= \frac{21.6\cdot 5.73\mu m + 5.4\cdot 5.065\mu m}{21.6 + 5.4}$$

$$= 5.597\mu m$$

The mass weighted average particle size in the bed, d_a, is

$$d_a = \frac{wt\%_{beads}(\text{bed})\,d_{beads} + wt\%_{clay}(\text{bed})\,d_{clay}}{wt\%_{beads}(\text{bed}) + wt\%_{clay}(\text{bed})}$$
$$= \frac{78.38 \cdot 775\mu m + 5.84 \cdot 5.597\mu m}{78.38 + 5.84}$$
$$= 722\mu m$$

The volume of kaolin in the slurry is $Vol_{kaolin} = Mass_{kaolin}/\rho_{kaolin} = (Mass_{slurry}/\rho_{kaolin})x(wt\%_{kaolin}/100)$. The volume of bentonite in the slurry is $Vol_{bentonite} = Mass_{bentonite}/\rho_{bentonite} = (Mass_{slurry}/\rho_{bentonite})x(wt\%_{bentonite}/100)$. The volume of NaCl in the slurry is $Vol_{NaCl} = Mass_{NaCl}/\rho_{NaCl} = (Mass_{slurry}/\rho_{NaCl})x(wt\%_{NaCl}/100)$. The volume of water in the slurry is $Vol_{water} = Mass_{water}/\rho_{water} = (Mass_{slurry}/\rho_{water})x(wt\%_{water}/100)$. The clay fraction in the slurry by volume is

$$Vol\%_{clay}(slurry) = 100Vol\%\frac{Vol_{Clay}}{Vol_{Total}}$$
$$= 100Vol\%\frac{\left(\frac{wt\%_{kaolin}}{\rho_{kaolin}} + \frac{wt\%_{bentonite}}{\rho_{bentonite}}\right)}{\left(\frac{wt\%_{kaolin}}{\rho_{kaolin}} + \frac{wt\%_{bentonite}}{\rho_{bentonite}} + \frac{wt\%_{NaCl}}{\rho_{NaCl}} + \frac{wt\%_{water}}{\rho_{water}}\right)}$$
$$= 100Vol\%\frac{\left(\frac{21.6}{2600} + \frac{5.4}{2795}\right)}{\left(\frac{21.6}{2600} + \frac{5.4}{2795} + \frac{0.1}{2165} + \frac{72.9}{998}\right)} = 12.29Vol\%$$

The clay fraction in the bed by volume is

$$Vol\%_{clay}(bed) = \frac{Vol\%_{clay}(slurry)}{100}Vol\%_{slurry}(bed) = \frac{12.29}{100}40.00Vol\% = 4.915Vol\%$$

The salt-water fraction in the bed by volume is

$$Vol\%_{salt-water}(bed) = 40Vol\%_{slurry}(bed) - 4.915Vol\%_{clay}(bed) = 35.08Vol\%$$

The corresponding void ratio in the packed bed is then

$$e = \frac{Vol\%_{salt-water}(bed)}{Vol\%_{beads}(bed) + Vol\%_{clay}(bed)} = \frac{35.08}{60.00 + 4.915} = 0.5405$$

Prior to testing, there were no measured data for the unconfined compressive strength of the Test 5 Scoping Study packed beds. Pretest predictions used the proposal from project document 24590-WTP-RPT-ENG-11-001, Rev 0, *Determination that Non-Newtonian Vessels Can Be Evaluated Using Newtonian Techniques* that the shear strengths for the packed cohesive, clay slurry/glass bead beds of the Test 5 Scoping Study might be approximated by the yield stress of the non-Newtonian clay slurry and that

the unconfined compressive strength might be approximated as twice this value thus UCS was estimated to be 2 x $\tau_{0,slurry}$ = 2 x 13.6 Pa = 27.2 Pa.

Using the Test 5 Scoping Study glass-beads/clay slurry bed parameters

- the carrier fluid density, $\rho_f = \rho_{slurry} = 1196$ kg/m^3,
- the carrier fluid dynamic viscosity, $\mu_f = \mu_{\infty,slurry} = 11.3$ cP = 0.0113 kg/(m s),
- the carrier fluid kinematic viscosity, $\nu_f = \nu_{\infty,slurry} = 0.0113/1196$ m^2/s = 9.45x10^{-6} m^2/s,
- the submerged specific gravity with respect to the carrier fluid based on the bed-averaged particle density, $s_a = (\rho_{beads} - \rho_f)/\rho_f = (2900$ kg/m^3 – 1196 kg/m^3)/1196 kg/m^3 = 1.425,
- the characteristic particle diameter for the solids in the packed bed based on the bed-averaged particle diameter, $d_a = d_{beads} = 722$ μm = 7.22x10^{-4} m, and
- the acceleration of gravity, g = 9.81 m/s^2

The pretest estimate for UCS* is calculated to be

$$UCS^* = \frac{UCS}{\rho_f s_a g d_a} \approx \frac{2 \cdot \tau_{0,slurry}}{\rho_f s_a g d_a} = \frac{27.2}{1196 \cdot 1.425 \cdot 9.81 \cdot 7.22\text{x}10^{-4}} = 2.25$$

Substituting Pc = 0.0584, e = 0.5405, and UCS*=2.25 into the Kothyari and Jain (2008) silt-sand correlation yields the pre-test prediction

$$\begin{aligned}\frac{\tau_{cc}}{\tau_c} &= 1.88\left(1+P_c\right)^{3/2} e^{-1/6}\left(1+0.001UCS^*\right)^{9/20} - 1.0 \\ &= 1.88\left(1+0.0584\right)^{3/2} 0.5405^{-1/6}\left(1+0.001 \cdot 2.25\right)^{9/20} - 1.0 \\ &= 1.27\end{aligned}$$

i.e. that the effect of cohesion was expected to be a 27% increase in the critical shear stress to mobilize the cohesive bed over the critical shear stress to mobilize the bed were it not cohesive.

A.7 Brownlie (1981)

For the glass-beads/clay-slurry beds in the Test 5 Scoping Study, the value of d* for use of the Brownlie (1981) model is

$$d^* = \left(\frac{s_a g}{\nu_f^2}\right)^{1/3} d_a = \left(\frac{1.425 \cdot 9.81}{\left(9.45\text{x}10^{-6}\right)^2}\right)^{1/3} 7.22\text{x}10^{-4} = 3.89$$

and shear strengths of the Newtonian

$$d^{*-0.9} = 3.89^{-0.9} = 0.2944$$

The critical value for the Shields parameter is

$$\theta_c = 0.22 d^{*-0.9} + 0.06 \exp\left(-17.73 d^{*-0.9}\right) = 0.22 \cdot 0.2944 + 0.06 \exp\left(-17.73 \cdot 0.2944\right) = 0.0651$$

The Brownlie (1981) estimate for τ_c is

$$\tau_c = \rho_f s_a g d_a \theta_c = \left(1200 \cdot 1.425 \cdot 9.81 \cdot 7.22 \text{x} 10^{-4} \cdot 0.0651\right) \text{Pa} = 0.7834 \text{Pa}$$

This estimate for the non-cohesive bed value of τ_c is within 100 x (0.7956 - 0.7834) / 0.7834 = 1.56% of the estimated value for the glycerol-glass beads bed. The pretest prediction for τ_{cc} using the Brownlie (1981) form of the Shields relations is

$$\tau_{cc} = \frac{\tau_{cc}}{\tau_c} (\text{from Kothyari and Jain, 2008}) \tau_c (\text{from Brownlie, 1981})$$
$$= 1.270 \cdot 0.7834 \text{Pa} = 0.995 \text{ Pa}$$

A.8 Cao, Pender, and Meng (2006)

For the glass-beads/clay-slurry beds in the Test 5 Scoping Study, the value of U_g for use of the Cao et al. (2006) model is

$$U_g = \sqrt{s_a g d_a} = \sqrt{1.425 \cdot 9.81 \cdot 7.22 \text{x} 10^{-4}} \text{m/s} = 0.1000 \text{ m/s}$$

The particle Reynolds number is

$$\text{Re}_p = \frac{U_g d_a}{\nu_f} = \frac{0.1000 \cdot 7.22 \text{x} 10^{-4}}{9.45 \text{x} 10^{-6}} = 7.64$$

The critical value for the Shields parameter is

$$\theta_c = \frac{\left[1 + \left(0.0223 \text{Re}_p\right)^{2.8358}\right]^{0.3542}}{3.0946 \text{Re}_p^{0.6769}} = \frac{\left[1 + \left(0.0223 \cdot 7.64\right)^{2.8358}\right]^{0.3542}}{3.0946 \cdot 7.64^{0.6769}} = 0.0815$$

The Cao et al. (2006) estimate for τ_c is

$$\tau_c = \rho_f s_a g d_a \theta_c = \left(1200 \cdot 1.425 \cdot 9.81 \cdot 7.22 \text{x} 10^{-4} \cdot 0.0815\right) \text{Pa} = 0.9810 \text{Pa}$$

This estimate for the value of τ_c were the glass beads/clay slurry bed non-cohesive is within 100 x (0.9838 - 0.9810) / 0.9810 = 0.29% of the estimated value for the glass beads/glycerol bed.

This estimate for the non-cohesive bed value of τ_c is within 100 x (0.9838 - 0.9810) / 0.9810 = 0.29% of the estimated value for the glycerol-glass beads bed. The pretest prediction for τ_{cc} using the Cao et al. (2006) form of the Shields relations is

$$\tau_{cc} = \frac{\tau_{cc}}{\tau_c}(\text{from Kothyari and Jain, 2008})\,\tau_c(\text{from Cao et al., 2006})$$
$$= 1.270 \cdot 0.9810\,\text{Pa} = 1.246\,\text{Pa}$$

Attachment 2
To
12-WTP-0216

TRANSMITTAL OF DEFENSE NUCLEAR FACILITIES SAFETY BOARD (DNFSB) RECOMMENDATION 2010-2 IMPLEMENTATION PLAN (IP) DELIVERABLES 5.3.3.1 AND CANCELLATION OF 5.3.3.2 AND 5.3.3.3

Determination that Non-Newtonian Vessels Can Be Evaluated Using Newtonian Techniques

Pages: 3 (including Coversheet)

Determination that Non-Newtonian Vessels Can Be Evaluated Using Newtonian Techniques

Document title:

Document number: 24590-WTP-RPT-ENG-11-001, Rev 1

Contract number: DE-AC27-01RV14136

Department: Mechanical Systems

Author(s): Joel Peltier

Checked by: Robert Hanson

Issue status: Issued for Cancellation

Approved by: L Russell Daniel

Approver's position: WCT Technical Manager

Approver's signature: Russell D Daniel (Signature) 5/30/12 (Date)

River Protection Project
Waste Treatment Plant
2435 Stevens Center Place
Richland, WA 99354
United States of America
Tel: 509 371 2000

History Sheet

Rev	Reason for revision	Revised by
0	For Issue	L. J. Peltier
1	For Cancellation	L. J. Peltier